Oxidation during the production of FGH4095 superalloy powders by electrode induction-melt inert gas atomization

Shan Feng(峰山), Min Xia(夏敏)[†], and Chang-Chun Ge(葛昌纯)[‡]

School of Materials Science and Engineering, University of Science and Technology Beijing, Beijing 100083, *China*

(Received 7 September 2017; revised manuscript received 12 December 2017; published online 10 March 2018)

Super-clean and super-spherical FGH4095 superalloy powder is produced by the ceramic-free electrode induction-melt inert gas atomization (EIGA) technique. A continuous and steady-state liquid metal flow is achieved at high-frequency (350 kHz) alternating current and high electric power (100 kW). The superalloy is immersed in a high-frequency induction coil, and the liquid metal falling into a supersonic nozzle is atomized by an Ar gas of high kinetic gas energy. Numerical calculations are performed to optimize the structure parameters for the nozzle tip. The undesired oxidation reaction of alloying elements starts at 1000 °C with the reaction originating from the active sites on the powder surfaces, leading to the formation of oxides, Me_xO_y. The role of active sites and kinetic factors associated with the diffusion of oxygen present in the atomization gas streams are also examined. The observed results reveal that the oxidation process occurring at the surface of the produced powders gradually moves toward the core, and that there exists a clear interface between the product layer and the reactant. The present study lays a theoretical foundation for controlling the oxidation of nickel-based superalloy powders from the powder process step.

Keywords: electrode induction-melt inert gas atomization (EIGA), powder metallurgy (P/M), FGH4095 superalloy powders, supersonic nozzle, oxidation

PACS: 47.45.Ab, 61.82.Bg, 68.08.–P, 68.35.Fx **DOI:** 10.1088/1674-1056/27/4/044701

1. Introduction

Powdered metals are the basis of powder metallurgy in a variety of applications including sintering and thermal spray coatings, and in aerospace, automotive, biomedical, and other areas.[1–4] Originally, the technique of powder metallurgy (P/M) was introduced for consolidating the superalloys to hinder them from being segregated, and also for fabricating the products with intricate shapes.[5] However, other problems such as gas porosity and undesired precipitation along previous particle boundaries (PPBs) were also found to occur in P/M superalloys.[6–9] There is a great interest in preparing the ultra-clean metal powders due to the extensive use of (P/M) superalloys in the production of high performance components in advanced gas engines.[6] Although the ceramic-free method of electrode induction-melt inert gas atomization (EIGA) is still a preferred technology for preparing the ultra-clean metal powders,[10–12] there is a necessity for further improving it and enhancing its efficiency. For example, Feng *et al.* have developed a Chinese-EIGA technique for preparing ultra-clean nickel-based superalloy powders.[13]

In general, special measures to be taken in the powder metallurgy processing of nickel-based superalloys in order to reduce the adverse effects of PPB precipitation.[14] The problem results from the surface contamination of the produced powders, where the contamination originates from oxidation during solidification due to surface adsorption.[15] In the EIGA technique using argon atomized FGH4095 powder, the reaction of alloying elements produces oxides and other by-products on the surfaces of the superalloy powders. The oxide-enriched surfaces of the powders have defects due to PPB at hot isostatic pressing (HIP), hot isothermal forging (HIF) and heat treatment (HT).[16] The defective PPB destroys the continuity of the matrix and causes the local stress to concentrate in a disk, and gives rise to an obvious influence on the mechanical properties, especially the low cycle fatigue (LCF) performance of the produced P/M superalloy, which later leads to the initiation of fatigue cracking and accelerates crack propagation under certain conditions, which in turn severely reduces the quality and reliability of the material.[9,17,18]

In this work, we study the advantages of immersing the superalloy electrode in a high frequency conical induction coil which induces an electro-magnetic field to heat the FGH4095 superalloy up to its melting temperature, yielding a continuous and steady-state liquid metal flow. Furthermore, we investigate the degree of oxidation and oxidation kinetics of the alloying elements in atomization and the formation of oxides on the surfaces of FGH4095 superalloy powders. This study also lays a theoretical foundation for the inhibition of the oxidation of FGH4095 superalloy powders and the reduction of defects arising from PPB. The theoretical results may also be useful in designing suitable parameters for controlling the ox-

[†]Corresponding author. E-mail: xmdsg@ustb.edu.cn
[‡]Corresponding author. E-mail: ccge@mater.ustb.edu.cn

© 2018 Chinese Physical Society and IOP Publishing Ltd

idation of nickel-based superalloy powders in the atomization process.

2. Experiment

2.1. Principle of induction melting and material properties

The working principle of the EIGA atomization technique is shown in Fig. 1. The FGH4095 superalloy electrode is immersed into a conical induction coil and a high-frequency electro-magnetic field, and induction melting was induced. The dimensions of the feedstock electrode are 40 mm in diameter and 500 mm in length for achieving a maximum feed rate of 100 mm/min.

In the induction melting process, the superalloy is heated from room temperature to a higher temperature. The chemical compositions of this FGH4095 superalloy are given in Table 1. Temperature-dependent physical properties of the melt superalloy, namely, the heat capacity (C_p), density (ρ), viscosity (μ), diffusivity (α), conductivity (λ), surface tension (σ), and resistivity (R) are used in the melting experiments. Listed in Table 2 are the physical properties of the superalloy at liquid temperatures.

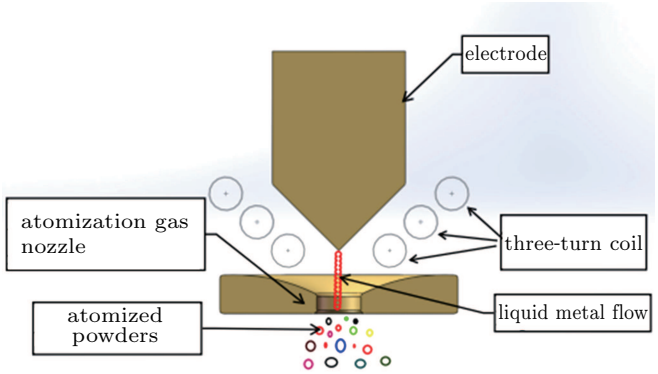


Fig. 1. (color online) Working principle of the EIGA atomization system.

Table 1. Chemical compositions of FGH4095 superalloy (wt.%).

C	Cr	Co	Mo	W	Al	Ti	Nb	Ta	Zr	Fe	B	Ni
0.06	12.24	8.54	3.65	3.46	3.525	2.46	3.49	0.01	0.03	0.43	0.0075	Bal.

Table 2. Physical properties at liquid temperature.

Heat capacity C_p/(J/g·K)	Density ρ/(g/cm^3)	Viscosity μ/mPa·s	Diffusivity α/(N/m)	Conductivity λ/(N/m)	Surface tension σ/(N/m)	Resistivity R/Ω·cm
0.413	8.03	5.5	4.243	14.010	1900	1.485×10^{-4}

2.2. Characterization and supersonic nozzle

A Mettler/Toledo TGA/DSC (1HT/1577) was used to analyze the oxidation characteristics of the FGH4095 superalloy powders in the atomization process. Confocal laser scanning microscopy (CLSM) was used to analyze the oxidized layers on the surfaces of superalloy powders. The finite element COMSOL Multiphysics®software was used to simulate the output parameters of the supersonic gas nozzle, and the nozzle shape is shown in Fig. 2. The compressible gas flow in the supersonic nozzle, and the gas flux are then considered to have a steady equal entropy flux, and therefore the numerical model is described by the continuity equations as follows:

$$\frac{\mathrm{d}\rho}{\rho}+\frac{\mathrm{d}u}{u}+\frac{\mathrm{d}A}{A}=0, \tag{1}$$

where ρ (in units kg/m^3) is the gas density in the atomization nozzle, u (m/s) is the gas velocity in the atomization nozzle, and A (m^2) is the cross sectional area of the atomization nozzle. The boundary conditions of the gas flow in the atomization nozzle can be written as

$$\begin{cases} \dfrac{T_2}{T_1}=\dfrac{1+\dfrac{K-1}{2}Ma_1^2}{1+\dfrac{K-1}{2}Ma_2^2}, \\ \dfrac{u_2}{u_1}=\dfrac{Ma_2}{Ma_1}\left(\dfrac{1+\dfrac{K-1}{2}Ma_1^2}{1+\dfrac{K-1}{2}Ma_2^2}\right)^{1/2}, \\ \dfrac{p_2}{p_1}=\left(\dfrac{1+\dfrac{K-1}{2}Ma_1^2}{1+\dfrac{K-1}{2}Ma_2^2}\right)^{k/(k-1)}, \\ \dfrac{\rho_2}{\rho_1}=\left(\dfrac{1+\dfrac{K-1}{2}Ma_1^2}{1+\dfrac{K-1}{2}Ma_2^2}\right)^{1/(k-1)}, \end{cases} \tag{2}$$

where T (K) is the temperature of gas in the atomization nozzle, u (m/s) is the gas flow velocity, p (Pa) is the pressure, and ρ (kg/m^3) is the density of gas flow. Compressible flows can be characterized by the value of the Mach number, Ma, which is given by

$$Ma=u/c. \tag{3}$$

Here, c (m/s) is the speed of sound in the gas, which is ex-

pressed as:

$$c = \sqrt{\gamma RT}, \tag{4}$$

where γ is the ratio of specific heats, R (8.314 J/mol·K) is the universal gas constant, and T (K) is the temperature.

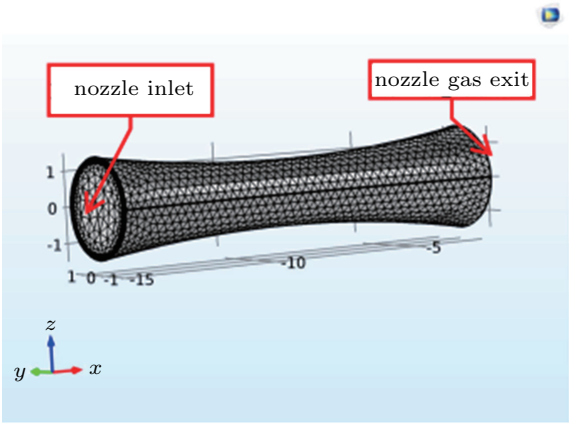


Fig. 2. (color online) Shape of supersonic gas nozzle.

3. Results and discussion

3.1. Optomization of induction melting power parameters

The optimization and selection of suitable induction melting parameters for producing the FGH4095 superalloy is an important step. The nickel-based superalloy displays various melting characteristics during melting. The melting viscosity of a nickel-based superalloy is high and the magnetic permeability of the material is low. The experimental process consists of two key steps, namely high frequency induction melting and the atomization of an inert supersonic gas. Figure 3(a) shows the melting experiment performed with a 350-kHz alternating current (AC) with an electric power of 100 K. In a typical experiment, the FGH4095 superalloy electrode is immersed into a conical induction coil. The high-frequency electromagnetic field produces an eddy current at the tip of the superalloy, which heats up and induces melting. Consequently, the liquid metal begins to flow downward along the tip of the superalloy electrode.

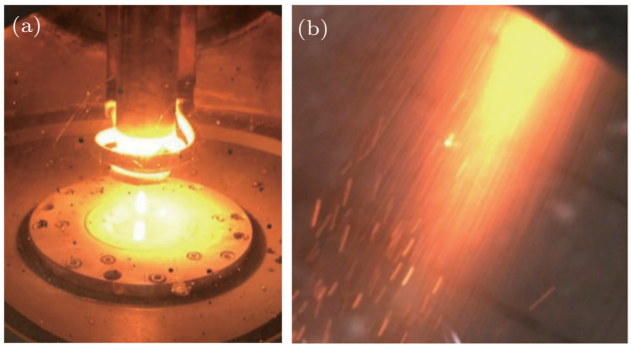


Fig. 3. (color online) EIGA process, showing (a) high frequency induction melting and (b) inert gas atomization.

As shown in Fig. 3(b), the liquid metal flows into a gas nozzle, where it is atomized with a stream of Ar gas having a high kinetic energy. This method possesses the induction melting characteristics of FGH4095 superalloy and other types of superalloy, and is conducive to obtaining a continuous and stable liquid metal flow. Thus, super-clean and super-spherical superalloy powders are produced by using the EIGA technique.

3.2. Oxidation of FGH4095 superalloy powders

The oxidation of superalloy powders is a complex chemical reaction in the EIGA atomization process. The TGA/DSC technique is employed to analyze the oxidizing of the FGH4095 superalloy powders during induction melting and inert gas atomization steps. The atmosphere of the TGA/DSC module is consistent with the atomization gas. Exact quantities of the superalloy powders (12.7713 mg) are adopted in the TGA/DSC module, and the thermal analyses are performed at an atmospheric pressure in a temperature range of 30 °C–1550 °C at a heating rate of 10 °C/min under a steady flow of Ar gas (50 Ml/min with the purity of 99.9%) for the complete oxidation. A representative TGA/DSC curve is shown in Fig. 4. As can be seen from the curve, the oxidation of alloying elements in the FGH4095 superalloy begins at 1000 °C with a gradual gain in mass. The average mass gain is about 23%. The relatively low concentration of oxygen in the inert atomization gas flow gives rise to oxidation resulting in a small increase in mass.

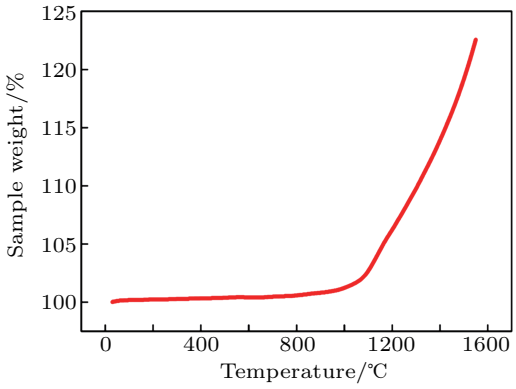


Fig. 4. (color online) TGA/DSC measurement curve showing the oxidative characteristics of FGH4095 superalloy powders.

The major oxides and other by-products formed in the atomization process are listed in Table 3. Equation (5) represents the oxidation reaction of the superalloy powder and equation (6) is used to determine the change in Gibbs free energy change (ΔG^0) as described below

$$\frac{2x}{y}\mathrm{Me} + \mathrm{O_2} = \frac{2}{y}\mathrm{Me}_x\mathrm{O}_y, \tag{5}$$

$$\Delta G^0 = -RT\ln K = A + BT. \tag{6}$$

The formation of metal oxides Me_xO_y and the oxidation of powder are related to ΔG^0 and temperature. The alloying elements have close affinities to oxygen in the processes of induction melting and gas atomization. On the basis of ΔG^0 values, the affinities of the alloying elements increase in the following order: Ni, Co, Fe, W, Mo, Cr, Nb, Ti, and Al close to the melting point of FGH4095 superalloy.

Table 3. The major oxides formed during the atomization process.

Oxidation reaction	A/J·mol^{-1}	B/J·mol^{-1}·k^{-1}	Temperature range/K
$4/3Cr + O_2 = 2/3Cr_2O_3$	–746800	170.3	298–2176
$2Co + O_2 = 2CoO$	–477800	173.2	298–1768
$2/3Mo + O_2 = 2/3MoO_2$	–448100	177.6	1068–1530
$2/3W + O_2 = 2/3WO_3$	–556500	158.6	298–1743
$4/3Al + O_2 = 2/3Al_2O_3$	–1120500	211.2	932–2345
$Ti + O_2 = TiO_2$	–943500	179.1	298–1940
$2Nb + O_2 = 2NbO$	–803300	158.6	298–2218
$2Fe + O_2 = 2FeO$	–519200	125.1	298–1642
$2Ni + O_2 = 2NiO$	–477000	168.6	298–1725

3.3. Degree of oxidation

The oxidation reation of the FGH4095 superalloy progresses from the liquid phase to a solidification phase of the reactant. The fine powder particles on the surface layers are more exposed to the gas flow than the cores of powder particles. In the supersonic gas atomization process, various degrees of oxidation layer occur on the surfaces of the powders as shown in Fig. 5. The oxidation reaction starts from the surfaces of powder particles, which then gradually moves toward the core, forming a clear interface between the product layer and reactant. The rapid solidification leads to the formation of an interfacial layer structure. Specifically, the oxidation reaction originates from the active surface sites of powder. Such active sites are marked as 1 and 2 (Fig. 6) and the entrance of oxidation into the core is determined by kinetic factors associated with the oxidation reaction of superalloy powders. The degree of oxidation (R) of the FGH4095 powder is given as follows:

$$R = \frac{m_0 - m}{m_0} = \frac{\frac{4}{3}\pi r_0^3 \rho - \frac{4}{3}\pi r^3 \rho}{\frac{4}{3}\pi r_0^3 \rho} = 1 - \left(\frac{r}{r_0}\right)^3, \qquad (7)$$

where m_0 (mg) is the original mass of powder, r_0 (μm) is the radius of original FGH4095 powder, m (mg) is the mass of unreacted core of the powder, r (μm) is the radius of unreacted core and ρ (kg/m^3) is the density of FGH4095 superalloy powder.

Figure 7 shows the oxidation process of FGH4095 powder, which can be divided into the following steps: the adsorbed oxygen on the surface of the FGH4095 powder and its external diffusion, the interfacial chemical reaction between oxygen and alloy elements, and the internal diffusion of oxygen passing through the reaction product layer. The internal diffusion rate J and the chemical reaction rate between the product layer and the interface u_c can be expressed as

$$J = -D_e A \frac{dc}{dt} = -4\pi r^2 D_e \frac{dc}{dt}, \qquad (8)$$

$$u_c = 4\pi r^2 k(c - c_{eq}), \qquad (9)$$

where k is the reaction rate constant (m/s), D_e is the effective diffusion coefficient (m^2/s), c is the oxygen concentration at the internal interface of reaction (mol/m^3), c_{eq} is the equilibrium concentration of reacting oxygen (mol/m^3), r is the radius (μm) of unreacted FGH4095 superalloy powder, t is the reaction time (s), and A is the interfacial surface area (m^2).



Fig. 5. (color online) Oxidation layers of FGH4095 powder.

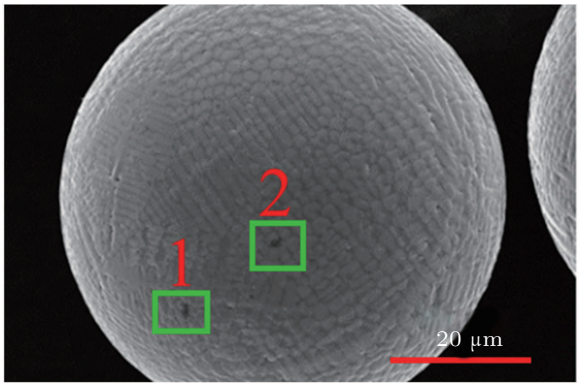


Fig. 6. (color online) Spots marked as 1 and 2 represent the active sites for the oxidation.

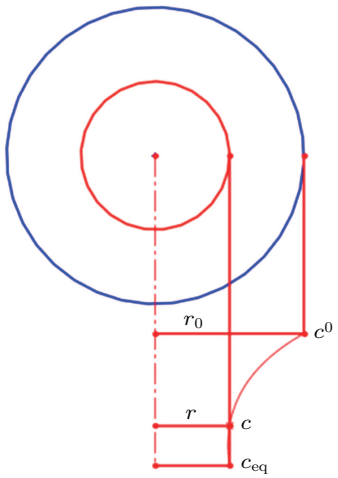


Fig. 7. (color online) Oxidation steps of FGH4095 powder.

3.4. Oxidation kinetics of atomization

The nozzle is critical in the atomization process as it can be used to control the break-up of the liquid melt, where the kinetic energy of Ar gas flow affects the oxidation of powders. A view of the gas atomization process using water is shown in Fig. 8 for easy visualization. The supersonic nozzle consists of four sections, namely, stable, convergent, throat and divergent. For successful atomization, it is necessary to optimize the structure factors of the nozzle. The structure factors calculated for the supersonic nozzle are shown in Fig. 9.



Fig. 8. (color online) Visualization of the water atomization process.

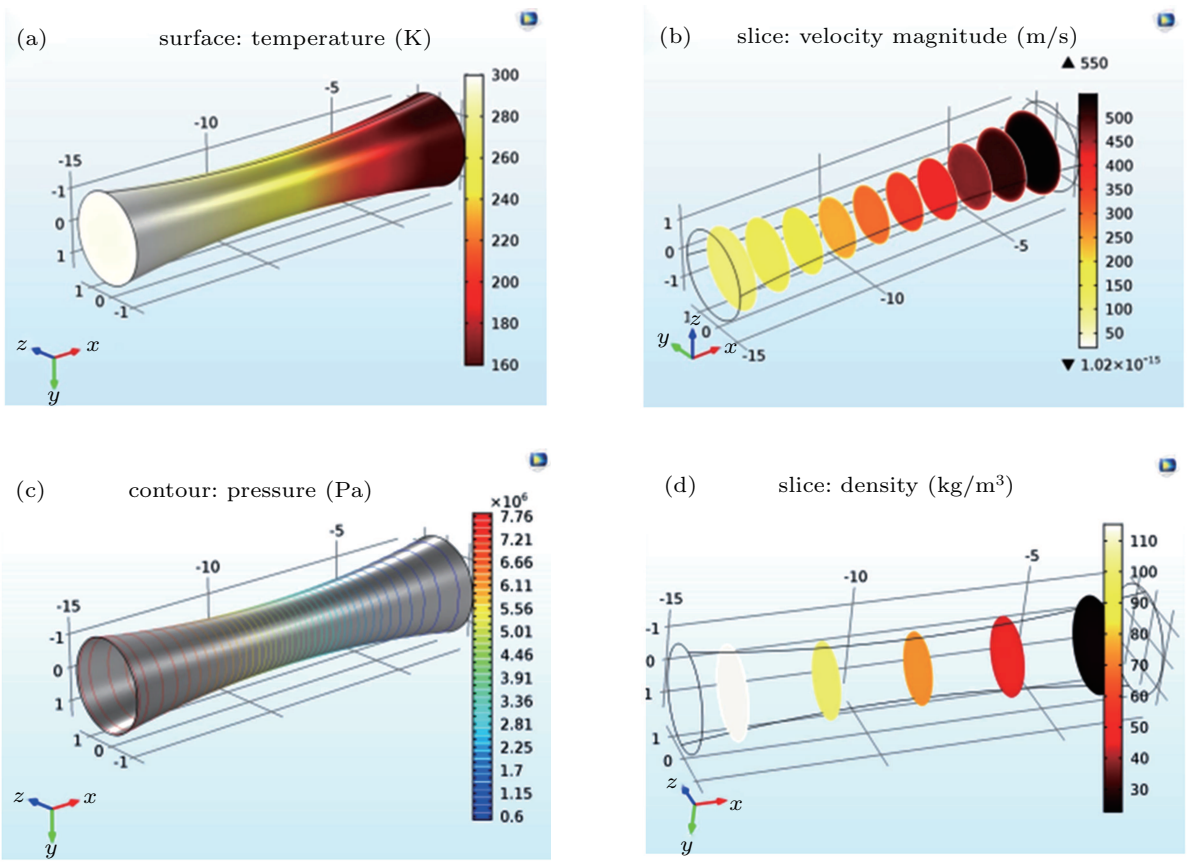


Fig. 9. (color online) Major structural parameters of supersonic nozzle: (a) temperature, (b) velocity, (c) pressure, and (d) density.

The inlet nozzle gas flow pressure is in a range of 4.0 MPa–8.0 MPa, and the gas purity is 99.9%. The various parameters for the supply pressure about 7.7 MPa of argon gas mass flow through the nozzle are numerically calculated, and they are an outlet temperature of 180 K, a velocity of 550 m/s, a pressure of 6.0×10^5 Pa, and a density 30 kg/m^3 at the exit of the supersonic nozzle. The parameters of the gas nozzle exit do not directly affect the liquid metal. The formation of gas flow from a supersonic gas jet is related to the distance between the exit of the nozzle and the liquid metal, and shown in Fig. 10. Upon contact with a supersonic gas jet the liquid metal is rapidly oxidized. The effect of atomization gas based

on the laws of energy and momentum conservation in this system, and the parameters of gas flow affecting the liquid metal can be calculated from the following equations:

$$\frac{u_{\text{exit}}^2}{2}+gz_{\text{exit}}+\frac{P_{\text{exit}}}{\rho_{\text{exit}}}=\frac{u_{\text{effect}}^2}{2}+gz_{\text{exit}}+\frac{P_{\text{effect}}}{\rho_{\text{effect}}}=\frac{1}{2}u_{\text{exit}}^2,$$
$$u_{\text{effect}}=u_{\text{exit}}\cdot\sin 35^\circ,\quad P_{\text{effect}}=P_{\text{exit}}\cdot\sin 35^\circ,$$
$$\rho_{\text{effect}}=\rho_{\text{exit}}\cdot\sin 35^\circ, \tag{10}$$

where u_{exit} (m/s) is the exit velocity at the nozzle, Z_{exit} (m) is the effective distance of liquid metal ($Z_{\text{exit}}=0$), P_{exit} (Pa) is the exit pressure at the nozzle, u_{effect} (m/s) is the effective velocity, Z_{effect} is the effective distance, P_{effect} (Pa) is the effective pressure, and ρ_{effect} (kg/m^3) is the effective gas density. The main parameter related to the oxidation kinetics in atomization is $E_{\text{oxidation}}$, which is defined as

$$E_{\text{oxidation}}=\frac{1}{2}u_{\text{effect}}^2. \tag{11}$$

In an atomization process, the oxidation Gibbs free energy can be expressed as

$$G=\Delta G^0+RT\ln\left(\frac{p_{\text{effect}}}{p^0}\right), \tag{12}$$

where G is the Gibbs free energy, ΔG^0 is the standard Gibbs free energy, T (K) is the induction melting temperature, P_{effect} (Pa) is the effective pressure, P^0 is the standard pressure (Pa) of oxygen in the atomization gas p^0 (1.00×10^5 Pa), and R is the gas constant ($R=8.314$ J/mol·K).

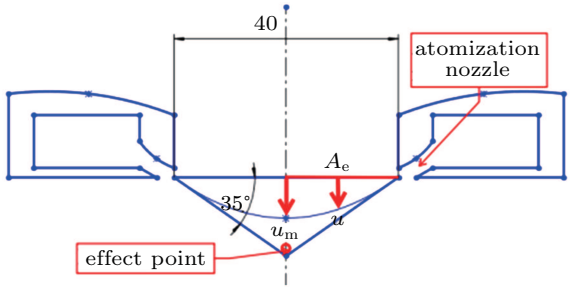


Fig. 10. (color online) Supersonic gas jet.

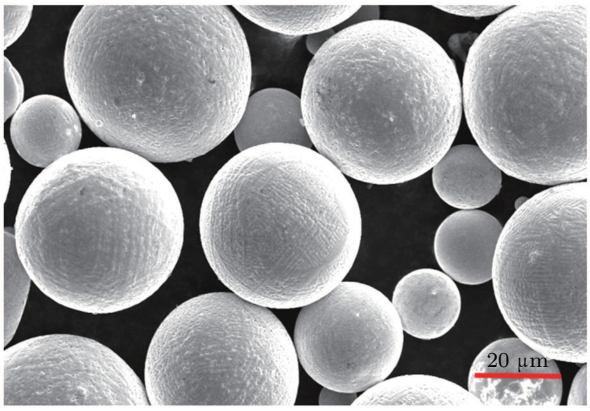


Fig. 11. (color online) Super-clean and super-spherical FGH4095 superalloy powders.

The applied parameters allow the atomization gas velocity to reach a supersonic speed, thereby enhancing the yields of superalloy powders and facilitating rapid solidification. Under the employed conditions the atomizing of super-clean and super-spherical FGH4095 superalloy powders is feasible by using the supersonic nozzle as shown in Fig. 11. These parameters lead to particle diameters in a range of 6 μm–120 μm. About 80% of the powders have particle diameters less than 50 μm, i.e., $d\leq 50$ μm which indicates a narrow size distribution.

4. Conclusions

In this work, the prepared super-clean and super-spherical FGH4095 superalloy powders are investigated by using the EIGA technique. The FGH4095 superalloy is inductively melted and subsequently a 350-kHz alternating current with an electric power of 100 kW are used to obtain a continuous and stable liquid metal flow. The alloying elements in the FGH4095 superalloy begin oxidizing at 1000 °C, with the gradual gain in mass. The formation of Me_xO_y oxides is closely related to the Gibbs free energy and induction melting temperature. The oxidation reaction originates from the active surface sites of the powder. The external diffusion and interfacial reaction of the oxygen on the surface of FGH4095 and its internal diffusion through the solid phase product layer also affect the degree of oxidation. The oxidation reaction gradually progresses from the surface to the core with forming the distinct interface between the oxide layer and unreacted core.

References

[1] Zeoli N, Tabbara H and Gu S 2011 *Chem. Eng. Sci.* **66** 6498
[2] Antony L V M and Reddy R G 2003 *JOM* **55** 14
[3] Belyanchikov L N 2008 *Russian Metallurgy* **2008** 588
[4] Bojarevics V Pericleous K and Cross M 2000 *Metallurgical and Materials Transactions B* **31** 179
[5] Na S, Yoon D, Kim J, Kim H and Kim D 2017 *Int. J. Fatigue* **101**, Part 1 27
[6] Ning Y Q, Zhou C, Liang H and Fu M W 2016 *Mater. Sci. Eng. A* **652** 84
[7] He G A, Liu F, Si J Y, Yang C and Jiang L 2015 *Mater. Design* **87** 256
[8] Crompton J S and Hertzberg R W 1986 *J. Mater. Sci.* **21** 3445
[9] Ma W B, Liu G Q, Hu B F, Zhang Y W and Liu J T 2013 *Mater. Sci. Eng. A* **587** 313
[10] Franz H, Plochl L and Schimansky F P 2008 *Proc. Titanium*
[11] Bojarevics V, Roy A and Pericleous K 2011 *COMPEL* **30** 1455
[12] Bernhard M and Geoffrey A M 1998 *Metal Powder Report* **53** 30
[13] Feng S, Xia M and Ge C C 2017 *Chin. Phys. B* **26** 060201
[14] Chang D R, Krueger D D and Sprague R A 1984 Superalloys 1984, *Proceedings of the Fifth International Symposium on Superalloys*, 1984 Ohio, USA, p. 245
[15] Yang W, Yu K, Yan M and Lai H 1992 *Adv. Mater. Proc.* **1** 339
[16] Wang X F, Zhou X M, Yang J, Zou J W and Wang W X 2013 *Mater. Sci. Forum* **747** 526
[17] Rao G A, Srinivas M and Sarma D S 2006 *Mater. Sci. Eng. A* **435** 84
[18] Coble R L 1978 *Powder Metall. Int.* **10** 128